Title

Influence of growth temperature on electrical, optical, and plasmonic properties of aluminum:zinc oxide films grown by radio frequency magnetron sputtering

Journal

Journal of Applied Physics, 114(14)

ISSN

00218979

Authors

Dondapati, Hareesh
Santiago, Kevin
Pradhan, A. K

Publication Date

2013-10-11

DOI

10.1063/1.4824751

Peer reviewed

Influence of growth temperature on electrical, optical, and plasmonic properties of aluminum:zinc oxide films grown by radio frequency magnetron sputtering

Hareesh Dondapati, Kevin Santiago, and A. K. Pradhan[a)]
Center for Materials Research, Norfolk State University, 700 Park Avenue, Norfolk, Virginia 23504, USA

(Received 9 August 2013; accepted 24 September 2013; published online 11 October 2013)

We have investigated the responsible mechanism for the observation of metallic conductivity at room temperature and metal-semiconductor transition (MST) at lower temperatures for aluminum-doped zinc oxide (AZO) films. AZO films were grown on glass substrates by radio-frequency magnetron sputtering with varying substrate temperatures (T_s). The films were found to be crystalline with the electrical resistivity close to $1.1 \times 10^{-3}\,\Omega\,\text{cm}$ and transmittance more than 85% in the visible region. The saturated optical band gap of 3.76 eV was observed for the sample grown at T_s of 400 °C, however, a slight decrease in the bandgap was noticed above 400 °C, which can be explained by Burstein–Moss effect. Temperature dependent resistivity measurements of these highly conducting and transparent films showed a MST at ~110 K. The observed metal-like and metal-semiconductor transitions are explained by taking into account the Mott phase transition and localization effects due to defects. All AZO films demonstrate crossover in permittivity from positive to negative and low loss in the near-infrared region, illustrating its applications for plasmonic metamaterials, including waveguides for near infrared telecommunication region. Based on the results presented in this study, the low electrical resistivity and high optical transmittance of AZO films suggested a possibility for the application in the flexible electronic devices, such as transparent conducting oxide film on LEDs, solar cells, and touch panels. © *2013 AIP Publishing LLC*. [http://dx.doi.org/10.1063/1.4824751]

I. INTRODUCTION

Transparent conducting oxides (TCO), such as, indium tin oxide (ITO) is being widely used as front electrodes in thin film based solar cell applications. Moreover, TCO have been received considerable attention from researchers due to their remarkable low resistivities and high transmittance in the visible region. ITO is one of the most commonly used TCO material because of its high transmittance in the visible region and resistivity close to $1.0 \times 10^{-4}\,\Omega\,\text{cm}$.[1,2] However, due to the fact of toxicity, high cost and moreover, thermal stability and diffusion barrier characteristics of ITO pose a problem for transparent electrodes in LEDs. Hence, one needs to be investigated for an alternative TCO material. Among all, unlike ITO, zinc oxide (ZnO) is nontoxic and inexpensive material. ZnO is a II–VI *n*-type semiconductor with a wide band gap of approximately 3.3 eV at room temperature and a hexagonal wurtzite structure. Since the exciton binding energy of ZnO is about 60 meV,[3] roughly three times larger than that of GaN, and the biexciton formation energy of ZnO is about 15 meV[3] also much larger than that of GaN, ZnO is considered to be a promising material for novel exciton-related devices. When III group impurities (e.g., Al and Ga) have been suitably added, then we can see a significant improvement in the electrical conductivity and the thermal stability of ZnO films.

It has been recently proposed that aluminum-doped zinc oxide (AZO) films can be the optimal choice as TCO layers in ZnO nanowire-based solar cells.[4,5] The bandgap of AZO can be tailored by changing the wt. % of Al_2O_3[6] in AZO films. Nb:TiO_2, which is transparent in the visible region and also shows a positive temperature coefficient of resistivity (TCR), has generated a lot of interest and excitement to understand the carrier generation and transport in highly conductive TCOs.[7] The electrical, optical, and structural properties of the doped ZnO films are influenced substantially by the deposition parameters in usual sputtering technique.[8] Furthermore, when n-type semiconductors are heavily doped with Al ion donors, the semiconductor shows a metal-like property in the resistivity, which follows ρ (resistivity) $\propto$ T (temperature).[9] The electrical and structural properties of Al:ZnO depending on the substrate temperature have been reported previously.[10,11] However, the influence of substrate temperature on their optical and plasmonic properties is not explored yet.

It was demonstrated that the doped degenerate wide-band gap semiconductors can be efficient nanoplasmonic as well as plasmonic photovoltaic materials in the near-infrared (NIR) spectral range because of strong confinement of surface plasmon polaritons (SPPs), low loss, and metallic behavior.[12–17] The compatibility of degenerate semiconductor, such as AZO with noble metals, is the carrier density and metal-like conductivity of AZO.[9] The plasma frequency, ω_{pl} predicted by the Drude theory as $\omega^2_{pl} = ne^2/\varepsilon_0 m_0{}^*$, where ε_0 is the permittivity of free space, e is the electron charge greatly depends on the carrier density. It remains very interesting to study the relation between the electrical conductivity as well as optical bandgap with the crossover frequency from positive to negative permittivity of AZO films containing varying Al content.

[a)]Author to whom correspondence should be addressed. Electronic mail: apradhan@nsu.edu

In order to understand the fundamentals of carrier generation and transport characteristics, which are related to the optical as well as plasmonic properties, we have investigated the temperature dependence of the resistivity of AZO thin films with varying substrate temperatures (T_s). We present structural, optical, electrical, and plasmonic properties in order to understand interesting characteristics of AZO films. The responsible mechanism for the observation of metallic conductivity at room temperature and metal-semiconductor transition (MST) at lower temperatures are studied in terms of donor characteristics and oxygen vacancies. Above all, the films demonstrate crossover in real permittivity, which is directly related to their optical and electrical properties. The AZO films demonstrate remarkable low loss in the NIR region.

II. EXPERIMENTAL DETAILS

Al-doped ZnO films were grown on corning glass substrates by the rf-magnetron sputtering technique from 2 wt. % Al doped ZnO target. All of the 7059 Corning glass substrates were cleaned in an ultrasonic bath with acetone and then methanol for 10 min. It is noted that the glass substrates were pre-annealed at 500 °C which is above their strain point of 480 °C in order to inhibit the film cracking. T_s varied from 300 °C to 500 °C with the increment of 50 °C at fixed rf power of 150 W and fixed Argon pressure of 2.3×10^{-3} Torr. The chamber was evacuated to a base pressure of 5×10^{-8} Torr, In order to make the films uniformity, the substrates were kept spinning during the sputtering. After etching away part of the film with diluted 10% HCl solution, thickness measurement of the films was performed using Dektak profilometer, and found to be between 270 nm to 290 nm. The X-ray diffraction (XRD) of the films was done in a Rigaku X-ray diffractometer using Cu Kα radiation. The atomic force microscopy (AFM) study of the surface roughness was performed using a Bruker dimension Icon AFM microscope. X-ray photoelectron spectroscopy (XPS) analysis was performed with a dual source VG Microtech XPS microprobe system using an Al X-ray (l = 1486.8 eV) source at 8×10^{-10} Torr with pass energy of 100 eV. The optical absorption and transmissions were measured by UV-VIS-IR spectrophotometer (Perkin Elmer Lambda 950 UVVIS-IR). The absorption was measured against a bare glass as a reference to obtain the absorption of the AZO films. Temperature dependence of the electrical resistivity was measured using a four-probe technique.

All AZO samples were measured by variable angle Spectroscopic ellipsometer (Model HS-190, J.A. Woollam Company). All permittivity values were taken from the scanning angle 70°. The probe wavelengths ranged from 1500 nm to 2500 nm in increments of 10 nm, and the scan angles were 65°, 70°, and 75°, resulting in over 300 data points per sample in which to model and calculate thicknesses and optical constants. Because of reduced measurement beam intensity due to film transparency, the high accuracy autoretarder was employed during measurement. It optimizes the light beam polarization prior to reaching the sample, producing the best measurement conditions for each sample.

III. RESULTS AND DISCUSSION

Fig. 1 shows XRD patterns of the AZO films grown on glass substrates, measured with conventional θ–2θ mode. All films gave a strong (0002) peak indicating polycrystalline with a hexagonal structure and had a preferred orientation with the c-axis perpendicular to the substrate. The only prominent peak observed in Fig. 1 is (0002) which is observed at $2\theta \sim 34.6°$ and is very close to that of the standard ZnO crystal (34.458). The absence of additional peaks in the XRD pattern excludes the possibility of any extra phases and/or large-size precipitates in the AZO films. The inset of Fig. 1 shows how full width at half maximum (FWHM) varies with various substrate temperatures. It is observed that FWHM decreases significantly from 0.36 to 0.26° as T_s increases from 300 °C to 400 °C.[18] However, it is clear that the AZO peaks become more intense as the T_s increases due to enhanced texturing of the films. On the contrary, FWHM bounces back to 0.30°, probably due to induced disorders caused by heavy Al doping or creations of Al_2O_3 clusters.

The surface morphology of AZO thin films was revealed by the AFM images as shown in Fig. 2. The AFM images of all the films present uniform distribution of grains. From Fig. 2(d) (for the sample grown at 400 °C), it is observed that dense distribution of bigger grains with well-defined boundaries, however, root mean square (RMS) is moderately low. It can also be seen that the roughness of the AZO thin films decreases from 3.36 nm to 1.60 nm as the substrate temperature rises from 300 °C to 450 °C. However, a slight increase in rms for the sample grown at T_s of 500 °C is noticed due to coalescence of grains. The AZO thin film with a surface roughness of ~2 nm is sufficient to meet the requirement for optical device applications. The interesting phenomena of dip and valley formations were observed for the samples grown at $T_s = 500$ °C, this probably due to pin-hole formation, consequently slightly increase in resistivity also observed in the resistivity section.

XPS studies were performed on all AZO films with varying the growth temperature. Figure 3(a) shows the

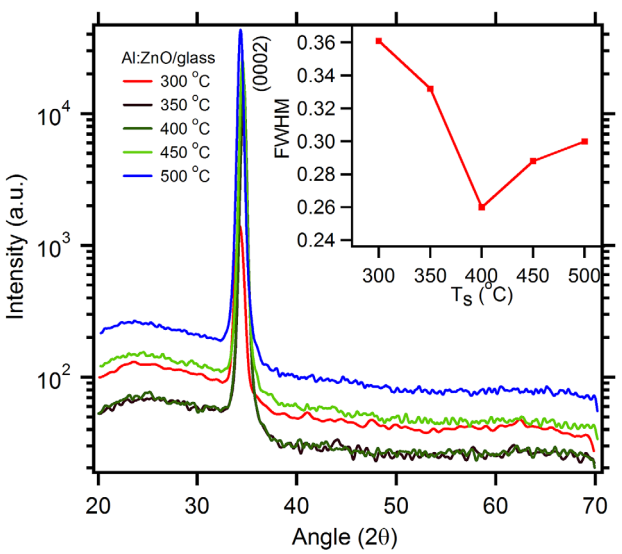

FIG. 1. XRD patterns of the AZO films at various substrate temperatures.

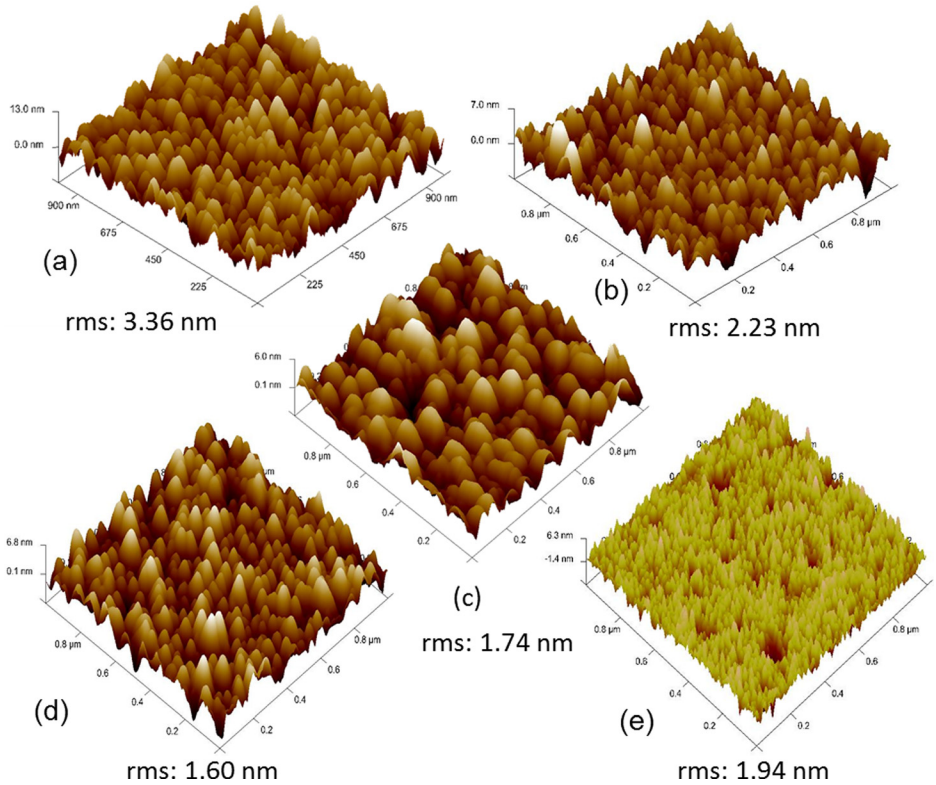

FIG. 2. AFM images of films surface (scan size $1\,\mu m \times 1\,\mu m$) grown at (a) 300 °C, (b) 350 °C, (c) 400 °C, (d) 450 °C, and (e) 500 °C.

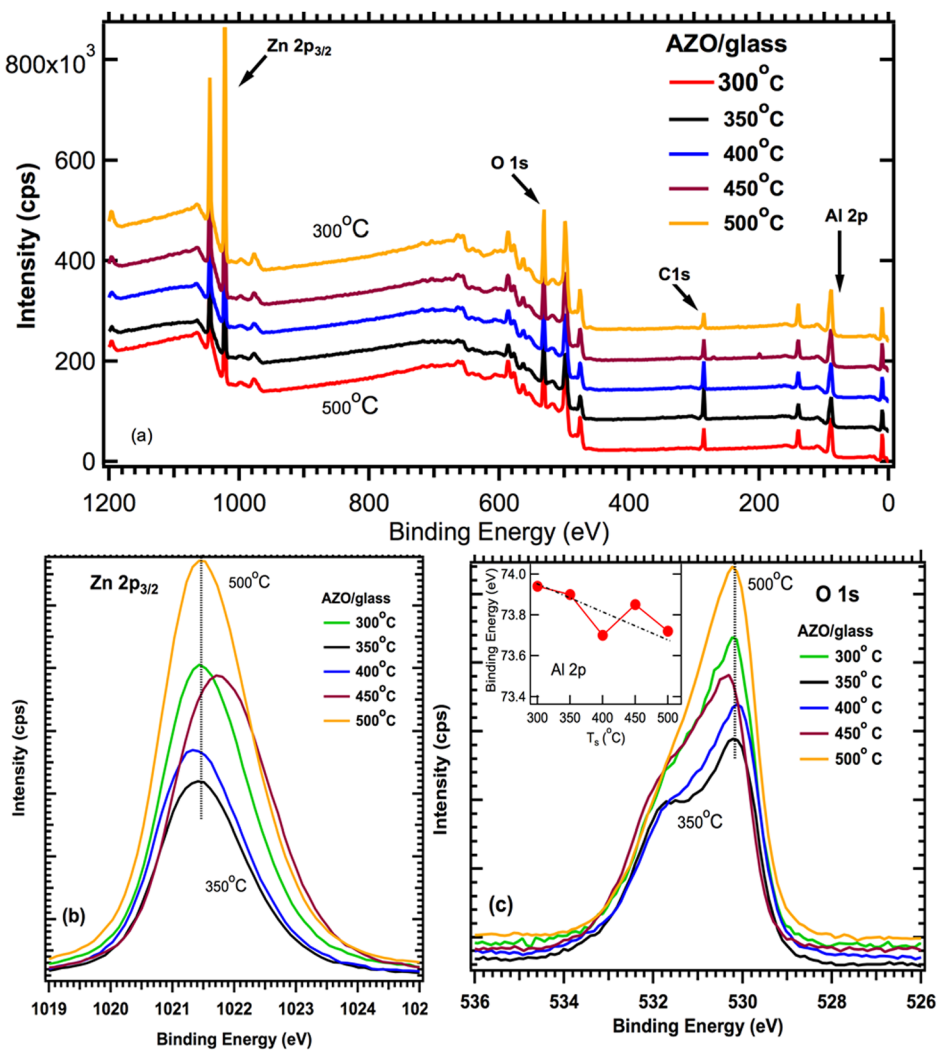

FIG. 3. XPS of AZO films (a) full range, (b) Zn $2p_{3/2}$, and O 1s spectra grown at various temperatures. The inset in (c) shows the growth temperature dependence of binding energy of Al 2p level.

typical XPS analysis of Zn, Al and oxygen peaks for AZO films grown at various temperatures. In Fig. 3(b), we have illustrated the influence of T_s on Zn $2p_{3/2}$, suggesting different degree of oxidation state in AZO films. Interestingly, it almost remains same for $T_s = 300$ and 500 °C. Figure 3(b) shows both O 1s as well as Al 2p peak position (inset) for Al-O bonding state, indicating higher Al-O bonding state for AZO films with various T_s values. It is expected that higher Al-O bonding (as evidenced by movement of the Al 2p peak to higher binding energy) in AZO films might induce Al_2O_3 clusters during the sputtering process when the films are grown at lower temperatures. In addition, the clear shifting of O 1s peak from higher energy to the lower energy state with a disappearance of hump is a clear indication of reduced oxygen related defect states at higher temperature, and confirms the higher oxidation state at lower growth temperatures. The Al atomic concentration increases from 0.6 to 0.8, 0.9, 1.1, and 1.5 as T_s increases from 300 °C to 350, 400, 450 and 500 °C, respectively. This clearly shows the formation of less free Al ions at lower T_s opposed to formation of Al_2O_3 clusters at higher T_s values.

The effect of doping was studied by measuring the electrical and optical properties of the films grown under different conditions. Fig. 4 represents the optical transmittance of AZO films deposited at various T_s in the wavelength range of 300–800 nm. The optical transmittance provides useful information about the optical band gap of the semiconductors. It was seen that the average transmittance of samples in the visible range was greater than 85%, which is an adequate value for transparent electrode application.

Dependence of optical absorption coefficient (α) on photon energy ($h\nu$) was examined to determine optical bandgap energy (E_g) of the AZO films. The relation of direct band gap energy with the absorption coefficient and photon energy is given[19,20] by the following equation:

$$\alpha h\nu = A(h\nu - Eg)^n, \quad (1)$$

where A is a constant, Eg is the band gap of the material, and n has different values depending on the optical absorption process. It was found that $n = 1/2$ is the best fit to our results, and is characteristic of the direct band absorption without phonon mediation. Fig. 5 shows the plot of $(\alpha h\nu)^2$ against $h\nu$ to obtain E_g of the films, and the sharp absorption edge can be accurately determined by linear fitting. It is noted that the band gap widens with increasing T_s from 300 °C to 400 °C and reached to its saturated value 3.76 eV at 400 °C. This is due to the fact that, with increasing substrate temperature results increasing carrier concentration and hence the conduction band will be partially filled, consequently the optical band gap, which is given by the energy separation between the valence band maximum and the lowest unfilled level in the conduction band, became widened, causing the absorption edge to shift toward the higher energy-side. Burstein[21] pointed out that the lifting of the Fermi level into the conduction band of the degenerate semiconductor leads to the energy band broadening (blue shift) effect. However, at very higher temperatures, such as above 400 °C, we observed a reverse trend in the bandgap, which is due to the fact that reduction in oxygen vacancies, probably facilitated by the creation of Al_2O_3 based clusters. This result is consistent with the FWHM results of X-ray as well as our XPS studies. Hence the absorption edge shifts toward longer wavelengths. The band gap decreases from 3.76 to 3.72 eV as T_s increases from 400 to 500 °C, this in contrast to our previous report on AZO grown the pulsed laser deposition technique.[22]

Fig. 6 shows the effect of T_s on the temperature dependence of electrical resistivity for AZO films. Fig. 6(a) corresponds to the films grown at two different T_s, such as 300 and 350 °C. It is noted that the sample grown at low temperature, such as 300 °C shows a semiconducting behavior, where we can see the negative TCR. This can be explained by taking an account of polycrystalline nature where the conduction electrons are more likely to be scattered by grain

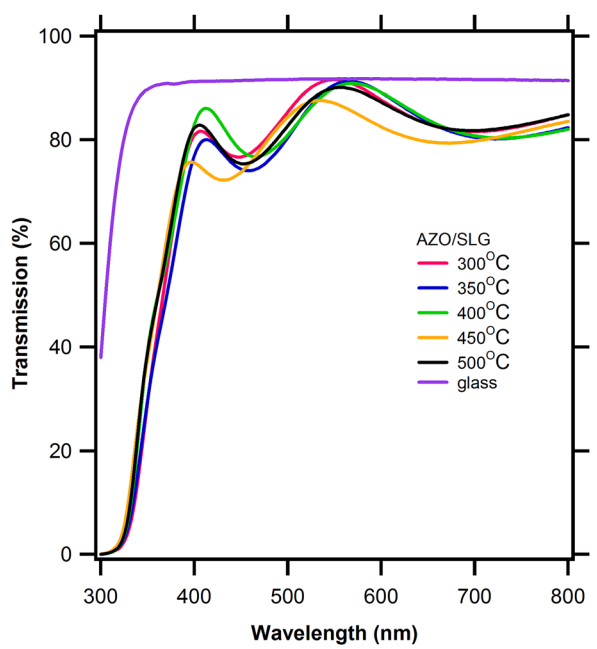

FIG. 4. Transmission spectra of AZO films in the wavelength range of 300–800 nm.

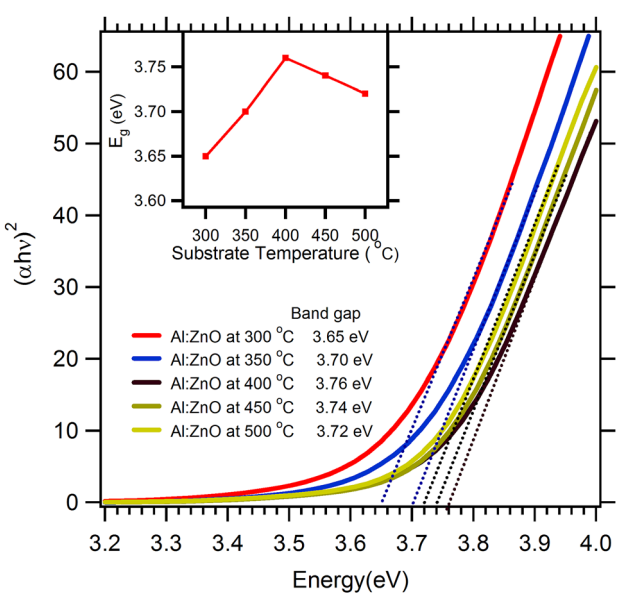

FIG. 5. Variation of band gap in AZO films deposited on glass substrates.

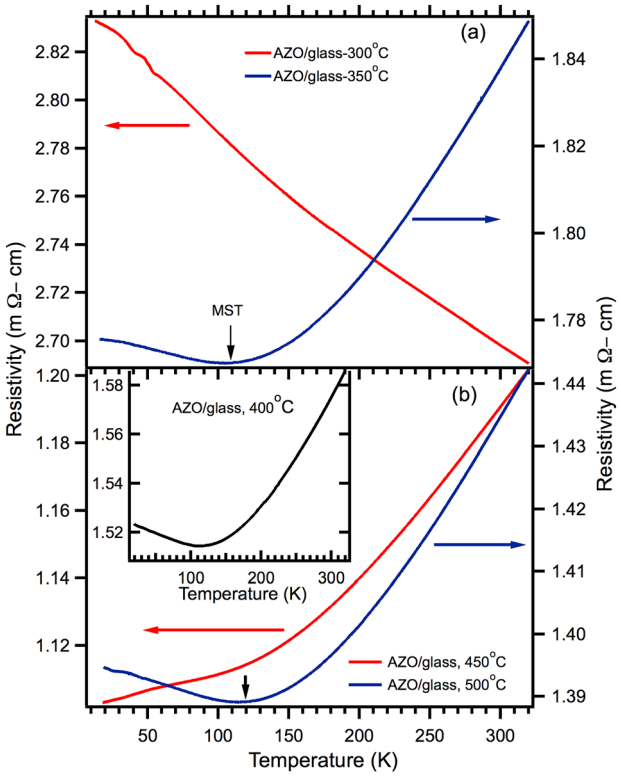

FIG. 6. Plot of resistivity vs. temperature for Al:ZnO films. The inset shows the resistivity vs. temperature for Al:ZnO films grown at 400 °C.

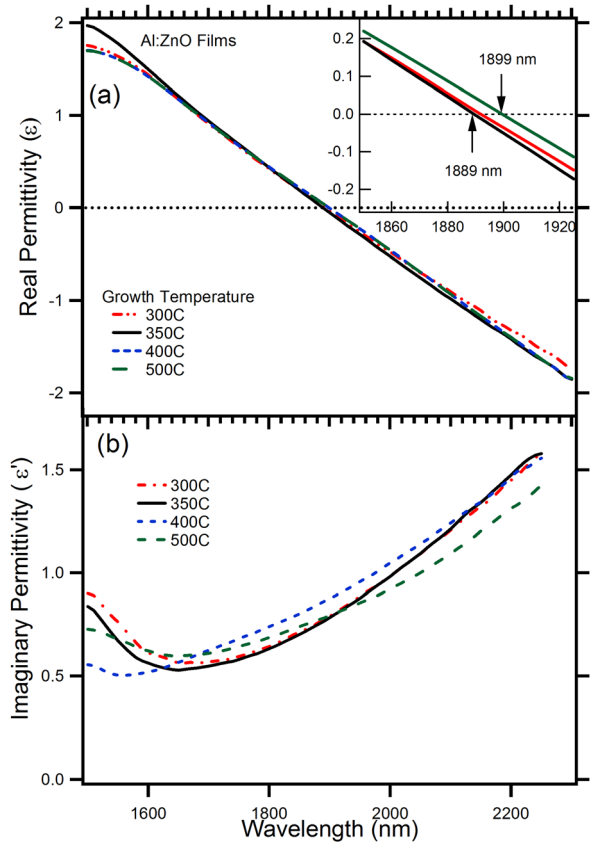

FIG. 7. (a) Real and (b) imaginary permittivity of Al:ZnO films grown at different temperatures. The inset in (a) shows the enlarged portion of the permittivity crossover.

boundaries.[23] This results in the highest resistivity, which is also confirmed by the presence of large grain boundaries from AFM data showed in Fig. 2(a). However, with the increment of T_s by 50 °C, all films started showing MST as seen in Figs. 6(b) and 5(c); metallic conductivity above ~110 K, and semiconducting behavior at temperatures below it. The metal-semiconductor transition increases from 115 K to about 120 K as T_s increases from 350 to 500 °C. The exception is that the film grown at 450 °C shows a typical metallic behavior. As temperature increases to 500 °C, the MST behavior returns back. The residual resistivity in such metallic films is related to the defects, especially due to oxygen vacancies and Al_2O_3 related clusters. A significant decrease in film resistivity may be achieved due to the removal of weakly bound oxygen species on the grain boundaries at higher T_s.[23]

The metallic conductivity observed here can be explained by the formation of a degenerate band appearing in heavily doped semiconductors as suggested by Mott.[20,24] However, the resistivity continues decreasing down to $T = 15$ K for $T_s = 450$ °C showing a characteristic residual resistivity behavior at low temperature which is generally found in an impure metal. This initial decrease in resistivity is due to the increase in free carrier concentrations at higher temperature that can be explained due to the Burstein–Moss effect.[25] However, with the further increase in T_s up to 500 °C the resistivity starts increasing. This is due to an increase in the concentration of the electron traps as a result of excess Al doping. Above the critical T_s as 450 °C, excess Al may introduce defects like the formation of non-stoichiometric Al_2O_3 clusters. These defects act as carrier traps rather than electron donors. The increased disorder of the crystal lattice causes phonon scattering and ionized impurity scattering,[26] resulting in increase in resistivity, which is further confirmed through our optical data where the bandgap slightly decreased from 3.76 eV to 3.72 eV. Moreover, at $T_s = 500$ °C surface morphology also reveals the formation of dip and valley which is very obvious for reduction in conductivity by grain boundary scattering.

Fig. 7 demonstrates the real and imaginary permittivity of Al:ZnO films grown at different temperatures. For permittivity measurements, all sputtered deposited films were measured by ellipsometry technique using J.A. Wollam ellipsometer model HS190. The nominal scan angles are 65, 70, and 75° in the scan range 1500–2500 nm with 10 nm increments. The resulting data points were modeled using software WVASE32 to infer real and imaginary permittivity. The main goal is to study the effects of carrier density on the plasma crossover frequency. As shown earlier, the electrical conductivity is a strong function of substrate temperature, and it is expected that there will be a change in permittivity due to change in carrier concentration. The permittivity changes sign from positive to negative in the NIR region for the films grown at all temperatures. The tunability is only 10 nm as shown in the inset in (a), which shows the enlarged portion of the permittivity crossover. However, the loss for all films is significantly low. Our results show a standalone AZO thin film with subwavelength thickness could be used for electro-optic modulator in the near infrared wavelength

region. Another advantage of AZO electro-optic modulator is its significantly low loss. As a plasmonic component, a tunable metal is very useful for nanophotonic device application. Both the free-electron plasma frequency and damping frequency of AZO can be adjusted by varying the Al-doping concentration.[27] Though these methods may tune the dielectric properties of the AZO film efficiently, they cannot change the dielectric property of a fabricated film in real time. The films fabricated by the rf magnetron sputtering with the current temperature range did not show any significant tuning of the crossover frequency by varying the growth temperature. This can be understood by following argument. The plasma frequency (i.e., related to the crossover frequency) is directly proportional to the electron density in the metal. However, a threshold electron density is necessary to observe the crossover wavelength in any plasmonic materials. It is very interesting to note that irrespective of a typical semiconductor behavior (as shown in Fig. 7(a)) for $T_s = 300\,^{\circ}\mathrm{C}$, a distinct crossover in real permittivity was observed at 1889 nm. In fact, all crossover wavelengths were observed with 10 nm in the NIR region. The electrical resistivity changes from 1.19 to 2.7 $\mathrm{m}\Omega\,\mathrm{cm}$ as T_s varies from 450 to 300 °C, and for $T_s = 500\,^{\circ}\mathrm{C}$, it is 1.435 $\mathrm{m}\Omega\,\mathrm{cm}$. With this boundary of resistivity (corresponding electron carrier density of $\sim 3 \times 10^{21}\,\mathrm{cm}^{-3}$), all current films show crossover frequency. Neither MST transition nor present growth temperatures (so as the surface rms) have strong impact on the crossover wavelength of AZO films grown by the sputtering technique even at a temperature as low as 300 °C. This is a significantly important result suggesting the use of this material for possible metamaterial applications.

IV. CONCLUSION

In summary, we have grown highly conducting and transparent aluminum-doped ZnO thin films on glass substrates by rf-magnetron sputtering. XRD measurements revealed that substrate temperature could enhance the crystallinity of ZnO thin films. For the AZO samples grown at 450 °C, the resistivity value is close to $1.1 \times 10^{-3}\,\Omega\,\mathrm{cm}$ and the transmittance is more than 85%. Such low resistivities and high transmittance were achieved with an optimized combination of dopant and oxygen vacancy concentration. All AZO films demonstrate crossover of the permittivity from positive to negative and low loss in the NIR region, illustrating its applications for plasmonic metamaterials, including waveguides for NIR telecommunication. Based on the results presented in this study, the low electrical resistivity and high optical transmittance of AZO films suggested a possibility for the application in the flexible electronic devices, such as transparent conducting oxide film on LEDs, solar cells, and touch panels.

ACKNOWLEDGMENTS

This work is supported by the NSF-CREST (CNBMD) Grant No. HRD 1036494, and DoD (CEAND) Grant No. W911NF-11-1-0209 (US Army Research Office). The authors would like to thank Rajeh Mundle for experimental help.

[1]T. Minami, MRS Bull. **25**, 38 (2000).
[2]T. Minami, Semicond. Sci. Technol. **20**, S35 (2005).
[3]A. Mang, K. Reimann, and St. Rübenacke, Solid State Commun. **94**, 251 (1995).
[4]M. H. Sukkar and H. L. Tuller, Adv. Ceram. **7**, 71 (1984).
[5]H. Porter, C. Mion, A. Cai, X. Zhang, and J. Muth, Mater. Sci. Eng., B **119**, 210 (2005).
[6]M. Tricot, C. Boulmer-Leborgne, and J. Perrière, J. Phys. D: Appl. Phys. **41**, 175205 (2008).
[7]Y. Furubayashi, T. Hitosugi, Y. Yamamoto, K. Inaba, G. Kinodo, Y. Hirose, T. Shimada, and T. Hasegawa, Appl. Phys. Lett. **86**, 252101 (2005).
[8]K. Ellmer, J. Phys. D: Appl. Phys. **33**, R17 (2000).
[9]O. Bamiduro, H. Mustafa, R. Mundle, R. B. Konda, and A. K. Pradhan, Appl. Phys. Lett. **90**, 252108 (2007).
[10]H. Kim, C. M. Gilmore, J. S. Horwitz, A. Piqué, H. Murata, G. P. Kushto, R. Schlaf, Z. H. Kafafi, and D. B. Chrisey, Appl. Phys. Lett. **76**, 259 (2000).
[11]K. H. Kim, K. C. Park, and D. Y. Ma, J. Appl. Phys. **81**, 7764 (1997).
[12]A. Boltasseva and H. A. Atwater, Science **331**, 290 (2011).
[13]Y. Tomita, C. May, M. Toerker, J. Amelung, M. Eritt, F. Loeffler, C. Luber, K. Leo, K. Walzer, K. Fehse, and Q. Huang, Appl. Phys. Lett. **91**, 063510 (2007).
[14]G. V. Naik and A. Boltasseva, Phys. Status Solidi (RRL) **4**, 295 (2010).
[15]M. A. Noginov, L. Gu, J. Livenere, G. Zhu, A. K. Pradhan, R. Mundle, M. Bahoura, Yu. A. Barnakov, and V. A. Podolskiy, Appl. Phys. Lett. **99**, 021101 (2011).
[16]A. K. Pradhan, T. Holloway, R. Mundle, H. Dondapati, and M. Bahoura, Appl. Phys. Lett. **100**, 061127 (2012).
[17]S. Pillai, K. R. Catchpole, T. Trupke, and M. A. Green, J. Appl. Phys. **101**, 093105 (2007).
[18]A. K. Pradhan, K. Zhang, S. Mohanty, J. B. Dadson, D. Hunter, J. Zhang, D. J. Sellmyer *et al.*, Appl. Phys. Lett. **86**, 152511 (2005).
[19]J. Tauc, in *Optical Properties of Solids*, edited by F. Abeles (North Holland, Amsterdam, 1970), Vol. 22, p. 903.
[20]E. A. Davis and N. F. Mott, Philos. Mag. **903**, 22 (1970).
[21]E. Burstein, Phys. Rev. **93**, 632 (1954).
[22]C. Fournier, O. Bamiduro, H. Mustafa, R. Mundle, R. B. Konda, F. Williams, and A. K. Pradhan, Semicond. Sci. Technol. **23**, 085019 (2008).
[23]S. O. Kasap, *Principles of Electronic Materials and Devices*, 3rd ed. (McGraw Hill, 2006).
[24]B. Y. Oh, M. C. Jeong, and J. M. Myoung, Appl. Surf. Sci. **253**, 7157 (2007).
[25]E. Burstein, Phys. Rev. **25**, 7826 (1982).
[26]M. Mizuhashi, Thin Solid Films **70**, 91 (1980).
[27]A. Frolich and M. Wegener, Opt. Mater. Express **1**, 883 (2011).